Available online at www.sciencedirect.com
ScienceDirect
Bioorganic & Medicinal Chemistry 14 (2006) 6307–6313
Bioorganic & Medicinal Chemistry

Towards NR2B receptor selective imaging agents for PET—synthesis and evaluation of *N*-[^{11}C]-(2-methoxy)benzyl (*E*)-styrene-, 2-naphthyl- and 4-trifluoromethoxyphenylamidine

Erik Årstad,[a,*] Stefan Platzer,[b] Achim Berthele,[b] Lyn S. Pilowsky,[c] Sajinder K. Luthra,[a] Hans-Jürgen Wester[d] and Gjermund Henriksen[d]

[a]*Hammersmith Imanet Ltd, Cyclotron Building, Du Cane Road, London W12 ONN, UK*
[b]*Department of Neurology, Klinikum rechts der Isar, Technische Universität München, Möhlstrasse 28,D-81675 Munich, Germany*
[c]*Institute of Psychiatry, KCL De Crespigny Park, London SE5 8AF, and Institute of Nuclear Medicine, UCL, Middlesex hospital, W1N 8AA, UK*
[d]*Department of Nuclear Medicine, Klinikum rechts der Isar, Technische Universität München, Ismaninger Strasse 22, D-81675 Munich, Germany*

Received 5 April 2006; revised 17 May 2006; accepted 24 May 2006
Available online 13 June 2006

Abstract—Three potent and selective ^{11}C-labelled NR2B antagonists have been synthesized and evaluated as PET ligands. The brain uptake of the compounds in mice varied substantially and was dominated by metabolism. One compound was found to have favourable uptake and retention in the brain, as well as a binding pattern consistent with the expression of the target receptor as measured by in vitro autoradiography. However, the metabolism of the compounds tested was too rapid to allow for in vivo imaging.

1. Introduction

N-methyl-D-aspartate (NMDA) receptors are a subtype of ligand-gated channels activated by the excitatory amino acid glutamate, which are highly permeable to Ca^{2+}. Their expression in the human CNS is widespread and they play a key role in a wide range of biological processes, including neuroplasticity, learning, memory, cognition, neuroprotection, as well as neurodegeneration.[1,2] In the diseased brain, glutamate-induced NMDA receptor-mediated hyperexcitation is linked to a variety of acute and chronic diseases, including stroke, neuropathic pain, schizophrenia and Parkinson's disease.[3,4]

It is well documented that NMDA receptors exist as tetrameric subunit assemblies made from both NR1 and NR2 receptor subunits.[4–7] The NR2 subunits (NR2A-D) give rise to four receptor subtypes, which have different pharmacological properties and expression patterns in the CNS. Of these, NR2A is expressed in most brain regions, most closely resembling the expression pattern of NR1. NR2C, which is most prominent in the cerebellum, and NR2D, which is highly expressed in midbrain and brainstem structures, are both sparse in cortical areas. In contrast, NR2B is most abundant in cerebral cortex, hippocampus and thalamic regions.[6,7]

The NR2B subunit is known to be involved in the pathophysiology of various disease states like schizophrenia, addiction and chronic pain,[4] and its regional distribution makes it particularly attractive for therapeutic intervention, since NR2B selective antagonists are less likely to adversely affect locomotor function compared with non-selective NMDA blockers. Positron emission tomography (PET) tracers targeting the NR2B receptor, by allowing non-invasive imaging in the living brain under these various disease states, could facilitate drug discovery and provide new diagnostic tools.

Over the last few years six compounds, CP 101,606,[8] BPDPO,[9] EMD95885,[10] two bis(phenyl)alkylamines[11] and Ro-647312[12] (Fig. 1), have been synthesized and evaluated as NR2B-selective PET tracers. Despite

Keywords: PET; NMDA-NR2B; Glutamate; Amidine; Carbon-11.
* Corresponding author. Tel.: +44 (0) 208 383 3714; fax: +44 (0) 208 383 2029; e-mail: erik.arstad@csc.mrc.ac.uk

0968-0896/$ - see front matter © 2006 Elsevier Ltd. All rights reserved.
doi:10.1016/j.bmc.2006.05.046

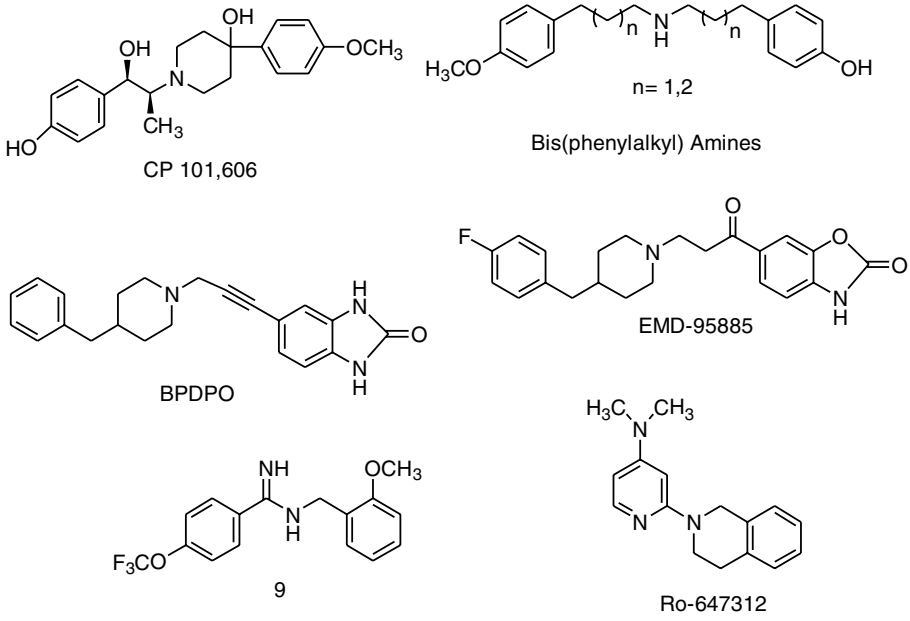

Figure 1. NR2B-NMDA selective antagonists.

promising results obtained in vitro, all compounds evaluated so far have suffered from low to moderate brain penetration and lack of NR2B-specific binding in vivo.

Recently, Merck published a new series of NR2B-selective compounds, based on the *N*-benzyl amidine structure. Within this series, several compounds were shown to have low to sub nanomolar affinities, high metabolic stability and high potency in vivo.[13,14] This suggests that the compounds readily cross the blood–brain barrier (BBB) and that their physiochemical properties can be tailored to meet the requirements for PET tracers. Recent publications in this field,[15] including reports[19,20] that the styrene and naphthyl derivatives [^{11}C]**7** and [^{11}C]**8** described herein are unsuitable as in vivo PET tracers, prompted us to publish our own results with this series of compounds.

The intention of this study was to evaluate whether the *N*-benzyl amidine class of compounds can form the basis for PET tracers for in vivo imaging of the NR2B-subtype receptors. Hence, three compounds were selected, that is, *N*-[^{11}C]-(2-methoxy)benzyl (*E*)-styrene-, 2-naphthyl- and 4-trifluoromethoxyphenylamidine, which combine structural diversity with the simplicity of [^{11}C]methylation for labelling.

2. Results and discussion

2.1. Chemistry

Commercially available nitriles **1**–**3** were treated with HCl gas in ethanol to give the corresponding imidates **4**–**6** in good to excellent yields (Scheme 1). Subsequent reactions with excess 2-methoxybenzylamine provided amidines **7**–**9**, which were obtained in good to high yields after crystallization. 2-Hydroxybenzyl amine was obtained by reducing 2-hydroxybenzamide with lithium aluminium hydride as described in the literature,[16] and subsequent reactions with imidates **4**–**6** in the presence of sodium methoxide gave the desmethyl precursors **10**–**12**.

2.2. Radiochemistry

Treatment of the precursors **10**–**12** with [^{11}C]methyl iodide in DMF in the presence of sodium hydride afforded the ^{11}C-labeled amidines **7**–**9** in 54–57% decay

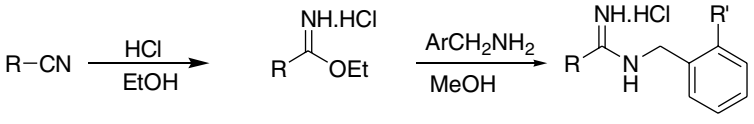

1 R = E-styrene
2 R = 2-naphthyl
3 R = p-$CF_3OC_6H_4$

4 R = E-styrene
5 R = 2-naphthyl
6 R = *p*-$CF_3OC_6H_4$

7 R = E-styrene, R' = OMe
8 R = 2-naphthyl, R' = OMe
9 R = *p*-$CF_3OC_6H_4$, R' = OMe
10 R = E-styrene, R' = OH
11 R = 2-naphthyl, R' = OH
12 R = *p*-$CF_3OC_6H_4$, R' = OH

Scheme 1. Synthesis of amidines.

corrected yield within 40 min after end-of-bombardment (EOB). The specific activity at end-of-syntheses (EOS) was >74 GBq/μmol for all compounds.

2.3. Biology

A good brain penetration is critical in neuroimaging both for providing a sufficient signal and to minimize radiation dose. As the lipophilicity of drugs often correlates with their initial brain entry, the octanol–water partition coefficient ($\log P_{oct/PBS}$) values for compounds **7**–**9** (Table 1) were measured. $\log P_{oct/PBS}$ was found to vary between 1.02 for compound **7** and 2.05 for compound **8**, with an intermediate value of 1.47 for compound **9**, suggesting that all three compounds should readily cross the blood–brain barrier (BBB). The brain uptake of compounds [^{11}C]**7**–**9** was subsequently measured in mice at 5, 20 and 40 min after iv injection (Table 1). The initial brain uptake of compounds **7** and **8** was moderate with approx 1% of injected dose per gram (%ID/g) measured in the brain 5 min after injection, while that of **9** was good with 1.8% ID/g. Interestingly, neither the brain penetration nor the retention therein correlates with the $\log P$ values or affinities of these compounds.

To assess the impact of metabolism on brain uptake, the composition of radioactive species in brain tissue was analyzed following injections of compounds [^{11}C]**7**–**9**. Radiolabelled species were extracted from brain homogenates with $\geqslant$90% efficiency and analyzed using radio-HPLC. The fraction of intact tracer for [^{11}C]**9** was 91 ± 2% at 5 min decreasing to 49 ± 7% ID/g at 40 min, whilst [^{11}C]**7** and [^{11}C]**8** were rapidly metabolized and at 5 min only 31 ± 4 and 37 ± 5% ID/g of the total activity corresponded to intact [^{11}C]**7** and [^{11}C]**8**, respectively. The remaining activity was identified as highly polar metabolites, which suggests that these species are formed within the brain and are unlikely to cross the BBB. Assuming that the metabolic rate measured in the brain reflects that in the periphery, the rapid metabolism of [^{11}C]**7** and [^{11}C]**8** compared to that of [^{11}C]**9** explains the discrepancy between lipophilicity and brain uptake for these compounds. If this is the case, derivatives with increased metabolic stability may have even higher brain uptake.

The presence of substantial amounts of metabolic species in the brain following injection of compounds [^{11}C]**7**–**9** prevented us from determining whether this class of compounds provides sufficient specific binding to the NR2B subunit for in vivo imaging. Instead, [^{11}C]**9** was chosen for further evaluation using in vitro autoradiography on rat brain sections. In these experiments, the binding pattern of [^{11}C]**9** was compared to that of [^{3}H]ifenprodil, a ligand with a conditional selectivity for NR2B-type receptors.[17] The binding pattern of [^{11}C]**9** was comparable to that obtained with [^{3}H]ifenprodil under conditions known to depict NR2B-sites, that is, enrichment in temporal cortex, caudate putamen, thalamus and in the hippocampal formation (Fig. 2). However, the binding of [^{11}C]**9** was higher in the caudate putamen and in the thalamus and less in the cerebellum, as compared with [^{3}H]ifenprodil. Since the NR2B subtype is poorly populated in cerebellum, the lower binding of [^{11}C]**9** in this region may indicate superior selectivity and specific binding. Quantification of the autoradiography data obtained with [^{11}C]**9** under no carrier-added conditions and in the presence of authentic **9** or ifenprodil revealed that its specific binding was higher than 75% for cortical regions, thalamus, caudate putamen and hippocampal formation (Fig. 3). The corresponding values for [^{3}H]ifenprodil were less

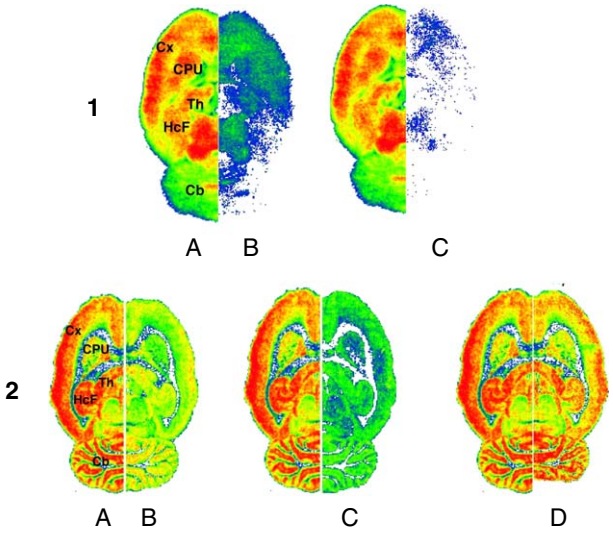

Figure 2. Autoradiography of rat brain sections incubated in vitro with no carrier added [^{11}C]**9** (1), under control conditions (1A), in the presence of 100 μM ifenprodil (1B) or in the presence of 100 μM authentic **9** (1C), compared with no carrier added [^{3}H]ifenprodil (2) under control conditions (2A), in the presence of 40 μM ifenprodil (2B) or in the presence of 100 μM authentic **9** (2C), or in the presence of 1 μM GBR 12909, GBR 12935 and (+)3-PPP (2D). Abbreviations: Cx, cortex; CPU, caudate putamen; Th, thalamus; HcF, hippocampal

Table 1. Lipophilicity, affinity, brain uptake and metabolism

Compound	$\log P_{oct/PBS}$[a]	K_i[b] (nM)	Brain uptake		% intact compd in brain		
			5 min[a,c]	40 min[a,c]	5 min[a]	20 min[a]	40 min[a]
7	1.02 ± 0.04	0.7	1.02 ± 0.23	0.37 ± 0.14	31 ± 5	16 ± 4	8 ± 3
8	2.05 ± 0.03	1.3	0.99 ± 0.27	0.78 ± 0.11	37 ± 4	21 ± 5	14 ± 5
9	1.47 ± 0.05	5.7	1.81 ± 0.12	1.13 ± 0.18	91 ± 2	80 ± 5	49 ± 7

[a] Data represent means ± SD, (n = 3–4).
[b] Data from references.[13,14]
[c] Radioactivity concentration is expressed as % of injected dose per gram tissue (% ID/g).

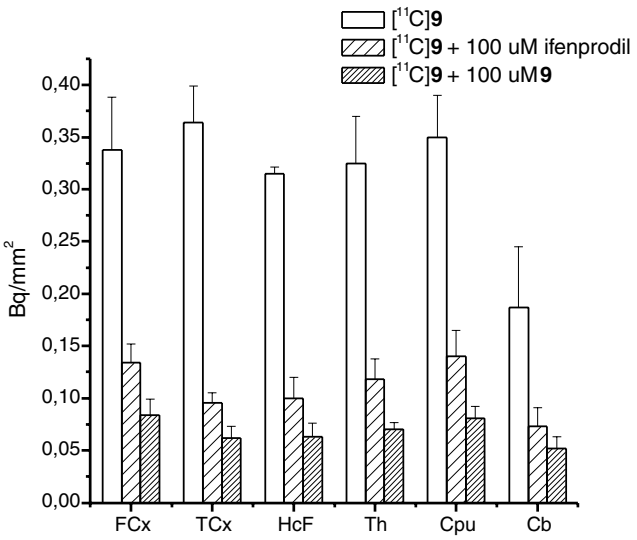

Figure 3. Quantification of binding of [^{11}C]**9** to rat brain sections incubated in vitro under control conditions and with 100 μM ifenprodil or 100 μM authentic **9**. Abbreviations: Cx, cortex; CPU, caudate putamen; Th, thalamus; HcF, hippocampal formation; Cb, cerebellum.

than 32% (data not shown). Overall, the autoradiography studies confirm that [^{11}C]**9** selectively binds to the NR2B subtype NMDA receptor. A receptor binding assay (by MDS Pharma Services, Taiwan) covering more than 30 receptors and subtypes[18] found no cross activity at 100 nM concentration, further supporting this conclusion. The differences observed between [^{11}C]**9** and [^{3}H]ifenprodil in the caudate putamen and in the basal ganglia in this work are noteworthy and require further investigation.

Although none of the compounds investigated have sufficient metabolic stability for in vivo imaging applications, our preliminary results suggest that the described ^{11}C-labelled *N*-benzyl amidines have a brain uptake suitable for PET imaging. In addition, one compound, [^{11}C]**9**, was found to have a specific binding in vitro in accordance with the distribution pattern of NR2B-containing NMDA receptors. Published SAR studies with this class of compounds have demonstrated that the required metabolic stability can be achieved, and the affinity retained, if appropriate substituents are introduced.[14] Taken together the results are highly encouraging and make us conclude that *N*-benzyl amidines should be further developed as NR2B-selective PET ligands.

3. Conclusion

Three ^{11}C-labelled, NR2B-selective compounds have been prepared and evaluated as potential PET-ligands. Within the series, the brain uptake varied substantially and was found to correlate with the metabolic rate of the compounds. One compound was found to have favourable uptake and retention in the brain, as well as a binding pattern consistent with the expression of the target receptor as measured by in vitro autoradiography. However, the metabolism of the compounds tested was too rapid to allow for in vivo imaging. Further optimization of this class of compounds may lead to successful PET tracers for the NMDA NR2B subtype receptor.

4. Experimental

4.1. General

All commercial reagents and solvents were used without further purification unless otherwise specified. Mass spectra were acquired under electron ionization (EI) conditions using a liquid chromatography mass spectroscopy system LCQ from Finnigan (Bremen, Germany) using the Hewlett Packard series 1100 HPLC system. ^{1}H NMR spectra were recorded on a JEOL ECP 500 (500 MHz) spectrometer, an AMX-400 (400 MHz) or an AMX-300 (300 MHz) spectrometer using the residual deuterated solvent signal as an internal standard. The chemical shifts are reported in ppm downfield from zero, and coupling constants are reported in hertz (Hz). Column chromatography was performed on a CombiFlash Companion (ISCO, Inc.) using RediSep normal phase disposable flash columns (Kieselgel). Analytical HPLC was performed using either a Nucleosil 100, 5 μm CN 4.6 × 250 mm reverse-phase column (CS-Chromatographie, Langerwehe, Germany) eluted with acetonitrile/0.1 M ammonium formate (55:45, v/v) mobile phase mixture or a Nucleosil 100, 5 μm C18 4.6 × 250 mm reverse-phase column (CS-Chromatographie) eluted with acetonitrile/0.1 M ammonium formate (65:35, v/v), and both systems were eluted at flow rates of 1.0 mL/min. Both chromatography systems were fitted with a UV detector (Sykam Model S3210 set at 254 nm; Sykam, Fuerstenfeldbruck, Germany). For detection of radioactive compounds, a γ-ray detector (Bioscan Flow-Count fitted with a NaI(Tl) detector) was used in series with the UV detector. Capacity constant, k', is calculated as follows: $k' = t_R - t_0/t_0$ where t_R = retention time and t_0 = dead volume of the column (mL)/flow (mL/min).

4.2. Syntheses of precursors for radiolabelling and reference compounds

4.2.1. Synthesis of ethyl cinnamimidate hydrochloride (4). HCl (gas) was bubbled through a solution of *trans*-cinnamonitrile (2.58 g, 20 mmol) in abs ethanol (2.25 g, 50 mmol) at −10 °C for 10 min. The resulting orange suspension was left in the cold for three days. To the resulting solid was added ether (10 mL) and the mixture was sonicated for 10 min. The tan solid was filtered off, washed with ether (10 mL) and dried to give the title compound (4.24 g, >95%). The product was used in the next reaction without further purification.

4.2.2. Synthesis of ethyl 2-naphthyl imidate hydrochloride (5). HCl gas was bubbled through a solution of 2-naphthyl nitrile (1.53 g, 10 mmol) in dichloromethane (10 mL) and EtOH (1.13 g, 25 mmol) at −10 °C for 15 min. The clear solution was left in the cold for two

weeks, at which time there was some formation of solids. The solvents were evaporated off, the residue washed with ether (10 mL) and filtered to give the product (2.09 g, 89% yield) as orange solid. The product was used in the next reaction without further purification.

4.2.3. Synthesis of ethyl 4-trifluoromethoxyphenyl imidate hydrochloride (6). This compound was prepared as described in the literature.[14]

4.2.4. General procedure for *N*-(2-methoxyphenyl)-amidine hydrochlorides. To a solution of the ethyl imidate hydrochloride (1.0 mmol) in MeOH (anhyd, 2 mL) was added 2-methoxybenzyl amine (2.0 mmol) and the mixture was stirred overnight. The solvents were evaporated off and the product mixture purified by crystallization.

4.2.5. Synthesis of *N*-(2-methoxyphenyl)-cinnamidine hydrochloride (7). The product mixture was crystallized from ethanol/ethyl acetate to give the title compound as white crystals (77%). ^{1}H NMR (CD_3OD, 400 MHz) δ 3.90 (s, 3H), 4.56 (s, 2H), 6.75 (d, J = 16.4 Hz, 1H), 7.02 (m, 2H), 7.35 (m, 2H), 7.45 (m, 3H), 7.63 (m, 2H) and 7.74 (d, J = 16.4, 1H): HRMS (ES+) *m/e* calcd for $C_{17}H_{19}N_2O$ (M+H) 267.1492; found, 267.1483.

4.2.6. Synthesis of *N*-(2-methoxyphenyl)-2-naphthyl amidine hydrochloride (8). The product mixture was crystallized from EtOH/acetone to provide the title compound as a tan solid (86%). ^{1}H NMR (DMSO-d_6, 300 MHz) δ 3.85 (s, 3H), 4.71 (s, 2H), 6.98 (t, 1H), 7.08 (d, 1H), 7.35 (m, 2H), 7.68 (m, 2H), 7.87 (d, 1H), 8.09 (m, 3H), 8.53 (s, 1H) and 9.94 (br, 3H); HRMS (ES+) *m/e* calcd for $C_{19}H_{19}N_2O$ (M+H) 291.1492; found, 291.1486.

4.2.7. Synthesis of *N*-(2-methoxyphenyl)-4-trifluoromethoxyphenyl amidine hydrochloride (9)[14]. The product mixture was crystallized from acetone to give the product as white crystalline material (77%). ^{1}H NMR (DMSO-d_6, 300 MHz) δ 3.84 (s, 3H), 4.65 (s, 2H), 6.96 (t, 1H), 7.07 (d, 1H), 7.34 (m, 2H), 7.60 (d, 2H), 7.95 (d, 2H) and 9.81 (br, 3H); HRMS (ES+) *m/e* calcd for $C_{16}H_{16}F_3N_2O_2$ (M+H) 325.1158; found, 325.1143.

4.2.8. General procedure for *N*-(2-hydroxyphenyl)-amidine hydrochlorides. To a mixture of 2-hydroxybenzyl amine[16] (0.330 g, 3 mmol) and NaOMe (0.130 g, 2.4 mmol) in MeOH (anhyd, 10 mL) was added the ethyl imidate hydrochloride (2.0 mmol) and the mixture was stirred overnight. The reaction was quenched by adding a solution of hydrochloric acid (concn, 1 mL) in MeOH (9 mL), the resulting mixture was filtered and the filtrate was concentrated in vacuo.

4.2.9. Synthesis of *N*-(2-hydroxyphenyl)-cinnamidine hydrochloride (10). The product mixture was purified by means of flash chromatography (silica, dichloromethane/MeOH gradient, 1% Et_3N) to give the title compound as a pale yellow solid (65% yield). The product contained traces of triethylamine, which could not be removed in vacuo. ^{1}H NMR (DMSO-d_6, 400 MHz) δ 4.43 (s, 2H), 6.76 (m, overlapping signals, 3H), 7.17 (m, 2H), 7.50 (m, 5H) and 7.82 (d, J = 16.4, 1H); HRMS (ES+) *m/e* calcd for $C_{16}H_{17}N_2O$ (M+H) 253.1335; found, 253.1336.

4.2.10. Synthesis of*N*-(2-hydroxyphenyl)-2-naphthyl amidine hydrochloride (11). The product mixture was purified by means of flash chromatography (silica, $CHCl_3$/MeOH/NH_3 9:1:0.1) to afford the title compound (54%) as a cream coloured solid.[1] ^{1}H NMR (DMSO-d_6, 300 MHz) δ 4.59 (s, 2H), 6.80 (t, 1H), 6.93 (d, 1H), 7.16 (t, 1H), 7.26 (d, 1H), 7.66 (m, 2H), 7.80 (d, 1H), 8.06 (m, 3H,), 8.42 (s, 1H) and 9.83 (br s, 3H); HRMS (ES+) *m/e* calcd for $C_{18}H_{17}N_2O$ (M+H) 277.1335; found, 277.1339.

4.2.11. Synthesis of *N*-(2-hydroxyphenyl)-4-trifluoromethoxyphenyl amidine hydrochloride (12). The product mixture was purified by means of flash chromatography (silica, $CHCl_3$/MeOH/NH_3 8.5:1.5:0.1) to give the title compound as a white solid (58%). ^{1}H NMR (DMSO-d_6, 300 MHz) δ 4.55 (s, 2H), 6.78 (t, 1H), 6.94 (d, 1H), 7.18 (m, 2H), 7.56 (d, 2H), 7.91 (s, 2H) and 9.78 (br s, 3H); HRMS (ES+) *m/e* calcd for $C_{15}H_{14}F_3N_2O_2$ (M+H) 311.1002; found, 311.0995.

4.3. Radiochemistry

Cyclotron produced [^{11}C]CO_2 was converted to [^{11}C]CH_3I by the catalytic gas-phase iodination reaction via [^{11}C]CH_4 (GE MeI MicroLab). Sodium hydride (4 mg; 0.21 mmol) was added to a vial containing the phenolic precursor (10 μmol) in anhydrous DMF (250 μl). The vial was sealed and was flushed with and maintained under argon. The [^{11}C]CH_3I produced, swept with a He-flow at 50 mL/min, was trapped in the reaction vial at −20 °C. The reaction vial was warmed to 45 °C over 30 s and kept at this temperature for 2 min. Thereafter the reaction mixture was diluted with 4 mL of 1.0 M ammonium hydroxide, loaded into a 7 mL injection loop and transferred onto a PRP-1 10 μm, 10 × 50 mm trace enrichment column (CS-Chromatographie) which was washed with water at a flow rate of 2 mL/min for 5 min and subsequently eluted in the reverse direction onto a μ-Bondapak 5 μm, 8 × 300 mm C18 column (CS-Chromatographie) by using a linear gradient of 15–70% B in 20 min; 0.1% TFA in water (A), 0.1% TFA in MeCN (B), flow rate 3 mL/min. In-line HPLC detectors included a UV detector (Sykam, set at 254 nm) and a γ-ray detector (Bioscan Flow-Count fitted with a PIN detector). For animal experiments, the fraction containing the product was collected in a rotary evaporation flask containing 1 mL of 1% HCl in EtOH and evaporated to dryness under reduced pressure. The product was dissolved in 1–5 mL of isotonic saline and transferred into a vial containing 0.1 mL of an 8.4% sodium bicarbonate solution. The pH of the final solution was between 7 and 8. Radiochemical and chemical purities were >95% as determined by analytical HPLC (k' = 2.8 using the CN analytical column eluted with 55/45 acetonitrile/0.1 M ammonium formate).

In the case of [^{11}C]**7** the radiochemical yield averaged 54% based on [^{11}C]methyl iodide and the specific activity averaged 76.4 GBq/μmol at end of syntheses

(EOS). The yields of [^{11}C]**8** and [^{11}C]**9** both averaged 57% with a specific activity of 77 and 81 GBq/μmol at EOS, respectively.

4.4. Lipophilicity measurements

Apparent drug lipophilicity was determined by a conventional partition method between 1-octanol phase and phosphate-buffered saline (PBS), pH 7.4. The 1-octanol was saturated with PBS before use. Briefly, to the non carrier added (n.c.a.) ^{11}C-labelled compound in question, contained in 4 mL PBS, was added 4 mL of 1-octanol in a 20 mL test tube. The tube was sealed and vigorously shaken at room temperature for 10 min. The mixture was then centrifuged at 3000*g* for 10 min. A 20 μl aliquot from each of the two phases were drawn and their radioactivity content was determined in a γ-counter. The $\log P_{\text{oct/PBS}}$ was calculated as follows:

$\log P_{\text{oct/PBS}}$ = log (radioactivity concentration in the 1-octanol phase/radioactivity concentration in the PBS phase). The reported values represent means of three independent measurements.

4.5. Biology

4.5.1. Biodistribution in Mice. Studies were performed in male Balb-C mice (body weight of 19–25 g). The mice were injected in a lateral tail vein with 10–20 MBq of a high specific activity (>37 GBq/μmol) ^{11}C-labelled amidine contained in <0.15 mL of a solution of isotonic saline. Groups of mice were sacrificed at 5–40 min post-injection. The radioactivity of weighed tissue samples was measured in a γ-counter. Data are expressed as percent of the injected dose per gram tissue (% ID/g) (means ± SD, $n = 3$–4). All animal studies were performed in accordance with the German law on protection of animals.

4.5.2. Metabolite analysis. Male Balb-C mice were injected with 15–32 MBq of the compound of interest. Five to forty minutes after injection the animals were sacrificed and the brain excised. Brain tissue homogenates were prepared immediately after dissection by mechanical homogenization of nitrogen-frozen samples followed by addition of 1 mL of phosphate-buffered saline. The mixture was vigorously vortexed, and 1 mL of MeCN was added. After centrifugation for 5 min at 6000*g*, the supernatant was collected. Approximately 0.1 mL of the supernatant solution was analyzed using radio-HPLC [Nucleosphere 100, 5 μm; 10 × 150 mm (CS-Chromatographie); MeOH/0.1 M ammonium formate 60:40 (v/v)]. The outlet of the column was connected in-line with a solid-phase scintillation counter (Flow-one Beta, Bioscan, Washington DC, USA). The amount of intact compound (I_c) was calculated as follows:

$I_c = [F_T/F_T + F_M] \times E_E \times E_R \times 1 \times 10^{-2}$, where F_T [%] represents the amount of intact tracer and F_M [%] the amount of metabolites as determined by radio-HPLC, corrected for extraction efficiency E_E [%] from the brain homogenates and the recovery E_R [%] of activity from the HPLC.

4.5.3. Autoradiography. Sections of rat brains (male, Wistar) were prepared by cryosectioning (20μm) and stored at −80 °C. [^{11}C]**9**: Unfixed frozen sections were thawed, dried and preincubated thereafter in 15 mM Tris–HCl buffer (pH 7.4) for 30 min followed by incubation with 25 nM [^{11}C]**9** (70 GBq/μmol) for 40 min at ambient temperature in an aqueous 50 mM Tris–HCl buffer (pH 7.4) without or in the presence of 100 μM authentic **9** or 100 μM ifenprodil. Subsequently, the sections were washed in 50 mM Tris–HCl for 5 min and dipped briefly in water. Finally the slices were dried under an air stream at 37 °C for 8–10 min and exposed to autoradiography film (Biomax MR, Kodak) for 6 h. [^{3}H]ifenprodil: After thawing and drying unfixed sections were preincubated in 15 mM Tris–HCl buffer (pH 7.4) for 30 min followed by incubation with 40 nM [^{3}H]ifenprodil (1.44 GBq/μmol) for 40 min at 0 °C in an aqueous 50 mM Tris–HCl buffer (pH 7.4). Non-specific binding of [^{11}C]**9** was determined in the presence of 100 μM authentic **9** or 100 μM ifenprodil. In separate experiments non-NMDA binding sites of [^{3}H]ifenprodil were masked with a 100 μM concentration of the σ-site ligand (+)-3-PPP, a 1 μM concentration of the dopamine blocker GBR-12909, and 1 μM concentration of GBR-12935 which blocks both dopamine uptake and piperazine sites.[21–23] The slices were washed and dried as described above for [^{11}C]**9** and exposed to autoradiography film (Kodak Biomax MR) for 8 weeks. To allow quantification of ligand binding tissue autoradiographs were digitized with a scanner (ArtixScan 2500f, Microtek, Hoogvliet, Netherlands). The scanner was calibrated as described elsewhere[24] and analyzed by using a computer-assisted image analysis system (Object-Image 2.10, http://www.simon.bio.uva.nl). Regions of interest were manually delineated on digitized scans. Measured optical densities were transposed to Bq/mm^2 by the calibration mode of the software.

Acknowledgment

Lyn S. Pilowsky was a UK Medical Research Council Senior Clinical fellow while this work was undertaken and has received speakers and consultancy fees from most of the major pharmaceutical companies.

References and notes

1. Kew, J. N.; Kemp, J. A. *Psychopharmacology (Berl)* **2005**, *179*, 4.
2. Perez-Otano, I.; Ehlers, M. D. *Trends Neurosci.* **2005**, *28*, 229.
3. Waxman, E. A.; Lynch, D. R. *Neuroscientist* **2005**, *11*, 37.
4. Loftis, J. M.; Janowsky, A. *Pharmacol. Ther.* **2003**, *97*, 55.
5. Laurie, D. J.; Bartke, I.; Schoepfer, R.; Naujoks, K.; Seeburg, P. H. *Brain Res. Mol. Brain Res.* **1997**, *51*, 23.
6. Rigby, M.; Le Bourdelles, B.; Heavens, R. P.; Kelly, S.; Smith, D.; Butler, A.; Hammans, R.; Hills, R.; Xuereb, J. H.; Hill, R. G.; Whiting, P. J.; Sirinathsinghji, D. J. *Neuroscience* **1996**, *73*, 429.

7. Scherzer, C. R.; Landwehrmeyer, G. B.; Kerner, J. A.; Counihan, T. J.; Kosinski, C. M.; Standaert, D. G.; Daggett, L. P.; Velicelebi, G.; Penney, J. B.; Young, A. B. *J. Comp. Neurol.* **1998**, *390*, 75.
8. Haradahira, T.; Maeda, J.; Okauchi, T.; Zhang, M. R.; Hojo, J.; Kida, T.; Arai, T.; Yamamoto, F.; Sasaki, S.; Maeda, M.; Suzuki, K.; Suhara, T. *Nucl. Med. Biol.* **2002**, *29*, 517.
9. Roger, G.; Lagnel, B.; Besret, L.; Bramoulle, Y.; Coulon, C.; Ottaviani, M.; Kassiou, M.; Bottlaender, M.; Valette, H.; Dollé, F. *Bioorg. Med. Chem.* **2003**, *11*, 5401.
10. Roger, G.; Dollé, F.; De Bruin, B.; Liu, X.; Besret, L.; Bramoulle, Y.; Coulon, C.; Ottaviani, M.; Bottlaender, M.; Valette, H.; Kassiou, M. *Bioorg. Med. Chem.* **2004**, *12*, 3229.
11. Sasaki, S.; Kurosaki, F.; Haradahira, T.; Yamamoto, F.; Maeda, J.; Okauchi, T.; Suzuki, K.; Suhara, T.; Maeda, M. *Biol. Pharm. Bull* **2004**, *27*, 531.
12. Dollé, F.; Valette, H.; Demphel, S.; Coulon, C.; Ottaviani, M.; Bottlaender, M.; Kassiou, M. *J. Labelled Compd. Radiopharm.* **2004**, *47*, 911.
13. Curtis, N. R.; Diggle, H. J.; Kulagowski, J. J.; London, C.; Grimwood, S.; Hutson, P. H.; Murray, F.; Richards, P.; Macaulay, A.; Wafford, K. A. *Bioorg. Med. Chem. Lett.* **2003**, *13*, 693.
14. Claiborne, C. F.; McCauley, J. A.; Libby, B. E.; Curtis, N. R.; Diggle, H. J.; Kulagowski, J. J.; Michelson, S. R.; Anderson, K. D.; Claremon, D. A.; Freidinger, R. M.; Bednar, R. A.; Mosser, S. D.; Gaul, S. L.; Connolly, T. M.; Condra, C. L.; Bednar, B.; Stump, G. L.; Lynch, J. J.; Macaulay, A.; Wafford, K. A.; Koblan, K. S.; Liverton, N. J. *Bioorg. Med. Chem. Lett.* **2003**, *13*, 697.
15. Hamill, T. G.; McCauley, J. A.; Burns, H. D. *J. Labelled Compd. Radiopharm.* **2005**, *48*, 1.
16. Zaugg, H. E.; Schaefer, A. D. *J. Org. Chem.* **1963**, *28*, 2925.
17. Nicolas, C.; Carter, C. *J. Neurochem.* **1994**, *63*, 2248.
18. The following receptors, channels and transporters were assayed: Adenosine-A1; adrenergic alpha 1 non-selective; adrenergic alpha-2 non-selective; adrenergic beta non-selective transporter; norepinephrine; calcitonin; calcium channel L-type; phenylalkylamine; calcium channel *N*-type, dopamine D_1; dopamine D_2L; dopamine D_2S; dopamine D_3; $GABA_A$ agonist site, benzodiazepine peripheral; $GABA_B$ non-selective; glutamate AMPA; glutamate NMDA agonism; glutamate NMDA phencyclidine; glutamate non-selective; histamine H_1; histamine H_2; histamine H_3; transporter—monoamine; muscarinic non-selective central; opiate non-selective; potassium channel [KATP]; serotonin 5-HT_1 non-selective; serotonin 5-HT_2 non-selective; $sigma_1$, $sigma_2$, sigma non-selective; sodium channel site 2.
19. (a) Thominiaux, C.; de Bruin, B.; Bramoulle, Y.; Hinnen, F.; Demphel, S.; Valette, H.; Bottlaender, M.; Besret, L.; Kassiou, M.; Dolle, F. *Appl. Radiat. Isot.* **2006**, *64*, 348–354; See also (b) Thominiaux, C.; deBruin, B.; Bramoulle, Y.; Hinnen, F.; Demphel, S.; Besret, L.; Bottlander, M.; Valette, H.; Kassiou, M.; Dollé, F. *J. Labelled Compd. Radiopharm.* **2005**, *48*, S179 (abstract).
20. Harahadira, T.; Fuchigami, T.; Fujimoto, N.; Okauchi, T.; Maeda, J.; Suzuki, J.; Suhara, T.; Yamamoto, F.; Mukai, T.; Maeda, M. *J. Labelled Compd. Radiopharm* **2005**, *48*, S92 (abstract).
21. Coughenour, L. L.; Cordon, J. J. *J. Pharmacol. Exp. Ther.* **1997**, *280*, 584.
22. Hashimoto, K.; Mantione, C. R.; Spada, M. R.; Neumeyer, J. L.; London, E. D. *Eur. J. Pharmacol.* **1994**, *266*, 67.
23. Schoemaker, H.; Allen, J.; Langer, S. Z. *Eur. J. Pharmacol.* **1990**, *176*, 249.
24. Berthele, A.; Platzer, S.; Jochim, B.; Boecker, H.; Buettner, A.; Conrad, B.; Riemenschneider, M.; Toelle, T. R. *Neuroimage* **2005**, *28*, 185.